

Library, L M A S

~~440221~~  
~~58~~  
~~10~~  
~~1~~

TECHNICAL MEMORANDUMS  
NATIONAL ADVISORY COMMITTEE FOR AERONAUTICS

No. 880

4.3.2.2  
4.5.1.1  
4.7.2.

THE EFFECTIVE WIDTH OF CURVED SHEET AFTER BUCKLING

By W. A. Wenzek

Luftfahrtforschung  
Vol. 15, No. 7, July 6, 1938  
Verlag von R. Oldenbourg, München und Berlin

Washington  
November 1938



NATIONAL ADVISORY COMMITTEE FOR AERONAUTICS

TECHNICAL MEMORANDUM NO. 880

THE EFFECTIVE WIDTH OF CURVED SHEET AFTER BUCKLING\*

By W. A. Wenzek

SUMMARY

The present report contains a description of experiments made for the purpose of ascertaining the effective width of circularly curved sheet under pure flexural stress.

A relation for the effective width of curved sheets is established. Comparisons with similar tests made by the DVL manifest good agreement.

I. INTRODUCTION

Experiments were made with circular cylinders compressed in longitudinal direction. The sheets were rigidly built in at the sides parallel to the axis of the cylinder. This should be borne in mind when applying the results to constructed airplane shells since frequently during riveting or by wide rivet pitch the sheet buckles at the stiffener sections also.

In stiffened shells under compression the carrying capacity of the buckled sheet between stiffeners can be accounted for by the introduction of an "effective width." The sheet is replaced by two assumedly buckling-resistant sheet strips of such width  $2 b_R$  that their carrying capacity under a stress equivalent to the shortening at the sheet edge is the same as that of the buckled sheet panel (fig. 1). For sheets rigidly built in at the side this stress is equal to the edge stress  $\sigma_R$  of the sheet.

$$\sigma_R 2 b_R = \sigma_m t \quad (1)$$

---

\*"Die mittragende Breite nach dem Ausknicken bei krummen Blechen." Luftfahrtforschung, vol. 15, no. 7, July 6, 1938, pp. 340-44.

To find the carrying capacity or the effective width  $2 b_R$ , respectively, circular brass cylinders were tested in pure compression conformably to figure 2. From the total load and the shortening of the section measured during the test, the section load (with allowance for the section shares) and the effective width of the sheet were obtained.

With unsymmetrically arranged stiffener sections which, aside from compression, are also subjected to small flexural stresses - say, due to eccentrically applied load for instance - the edge stress  $\sigma_R$  and the mean section stress  $\sigma_{mp}$  manifest considerable discrepancies under certain circumstances. In such cases, it is preferable to refer the value for the effective width for practical reasons by  $\frac{\sigma_R}{\sigma_{mp}}$  to the mean section stress:

$$2 b_{mp} = \frac{\sigma_R}{\sigma_{mp}} 2 b_R = F_1 \left( \frac{\sigma_R}{\sigma_k} \right) F_2 \left( \frac{\sigma_R}{\sigma_k} \right) \quad (2)$$

## II. RESULTS

The effective width of the flat sheet in pure compression is, according to Lande-Wagner (reference 1)

$$\frac{2 b_R}{t} = k \sqrt{\frac{\sigma_k}{\sigma_R}} \quad (3)$$

whereby a slightly exceeded buckling stress  $\left( \frac{\sigma_R}{\sigma_k} < 3 \right)$  is presumed for  $k = 1$ . By considerably exceeded buckling stress  $\left( \frac{\sigma_R}{\sigma_k} > 3 \right)$   $k$  ultimately approaches 2. The factor  $k$  was obtained from experiments on sheets with rigidly built-in edges.

On the basis of these tests, the equation for the effective width of circularly curved sheets is as follows

$$\frac{2 b_R}{t} = \sqrt{\frac{\sigma_k}{\sigma_R}} - \varphi \left( 1 - \frac{\sigma_k}{\sigma_R} \right) \quad (4)$$

where  $\varphi = \frac{t}{r}$  is the angle at center of the sheet panel,

$\sigma_R$ , the edge stress appearing at the edge of the sheet, and

$\sigma_k = \sigma_{eb} + \sigma_{kr} = 5 E \left( \frac{s}{t} \right)^2 + 0.3 E \left( \frac{s}{r} \right)$  is the buckling stress of the panel.

The values for  $\frac{2 b_R}{t}$  are plotted in figure 3 for the flat sheet according to equation (3) and for the curved sheet ( $\varphi$  up to  $30^\circ$ ) according to equation (4) against the degree of exceeded buckling load  $\left( \frac{\sigma_R}{\sigma_k} \text{ up to } 13 \right)$ .

In the extreme case of  $\varphi = 0$ , equation (4) becomes equation (3) for the flat sheet provided that the buckling stress is not substantially exceeded  $\left( \frac{\sigma_R}{\sigma_k} < 3, \text{ i.e., } k = 1 \right)$ . Otherwise  $\left( \frac{\sigma_R}{\sigma_k} > 3 \right)$  we find  $k > 1$  for the flat sheet according to Wagner-Lahde's tests; and in this case the curved sheet, equation (4) does not change to the flat sheet, equation (3). Within the zone of very small  $\varphi$  rigidly built-in sheets probably disclose marked sensitivity relative to original curvatures.

Equation (4) is applicable to sheets with built-in longitudinal edges under pure compression. For the panel edge diagonal to the direction of compression, the experiments disclosed no noticeable impairment of the wrinkling condition as a result of the clamping effect, on tolerably great panel length  $l$  to panel width  $t$  ( $l/t > 2.5$ ).

With regard to the range of the dimensions, equation (4) applies only to such dimensioned sheets as at buckling manifest elastic strains.

Figure 4 illustrates the results of a calculation of the effective width for the same edge stresses according to equation (4) plotted against the angle at the center  $\varphi$ . The data refer to brass sheets of given aspect ratio  $\left( \frac{t}{s} = 500 \right)$ . The effective width grows, as is seen, almost proportionally with  $\varphi$  in the plotted range. Only at high

edge stresses does an almost complete flattening-out of the lines take place. A means of comparison between the carrying capacity of flat ( $\phi = 0$ ) and curved sheet is afforded by the dashed line; its location complies with the condition  $2 b_R(\text{curved}) = 2 b_R(\text{flat})$ .

### III. TEST SPECIMENS AND TEST LAY-OUT

Altogether, eleven test cylinders of springy sheet brass\* were provided. The panels were riveted together by copper rivets with a 2 cm pitch at the lap-riveted seams and 3 cm at the sections (fig. 2). Against undesirable wrinkling of the sheet edge a symmetrical arrangement of the flanged sections and flattened sheet edges provided in some measure a guarantee for the zones of maximum compression stress as well. To forestall an adverse load initiation, the test specimen and the pressure plate of the experimental set-up were mutually fitted in to about 7/1000 mm under light-slot control by luminous bodies mounted in the cylinder.

The choice of cylinder dimensions was largely governed by the customary range of application in airplane shell construction.

Table I contains the most important cylinder dimensions, the individual  $\phi$ ,  $\frac{r}{s}$ , and  $\frac{t}{s}$  values as well as cross-section proportions of section and sheet, along with the theoretical and experimental buckling-stress data.

The test lay-out (fig. 5) consists of two pressure plates whose distance can be varied as desired by a spindle. To assure purest possible compression stresses, a flexible tension bar a was mounted at the lower end of the spindle and the lower pressure plate was fitted with a longitudinal ball bearing. The test load was computed from the measured sag of two springs c mounted on knife edges b, figure 6. The instrumental accuracy was around 1 percent within the range of 600 to 10,000 kg.

---

\*Elongation (strain) measurements on cylinders 4, 6, 7, and 8 averaged  $E = 1.03 \times 10^6$  kg/cm<sup>2</sup>, and  $E = 1.06 \times 10^6$  kg/cm<sup>2</sup> for the others.

## IV. TEST PROCEDURE AND INTERPRETATION

The test cylinders were progressively loaded to failure, i.e., to the highest admissible stress of the test lay-out. The compressive strain  $\epsilon_p$  in the sections was recorded on three dial gages (figs. 8 to 12). The readings were simultaneous and afforded good agreement before and after buckling.

The evaluation of the measurements was as follows: from the difference of total load  $P_Q$  and section load  $P_P = 3 \epsilon E F_P$  the load supported by the sheet was obtained after which with consideration to the sheet area  $F_B = 3 s t$  the effective width was computed at

$$2 b_R = \frac{3 P_B 3 F_P}{3 F_P 3 F_B} t$$

Figure 7 illustrates the test data for the effective width arranged according to  $\phi$ . The experimentally defined values for  $\frac{2 b_R}{t}$  (single dots) and those computed according to equation (4) (solid line) are shown plotted against the degree of exceeded theoretical buckling load  $\left(\frac{\sigma_R}{\sigma_k}\right)$ .

## a) Buckling Stress of Sheet Panel

Buckling occurred simultaneously on all three panels. The experimental buckling stresses are in good agreement with the theoretical values

$$\left(\sigma_k = \sigma_{e_b} + \sigma_{kr} = 5 E \left(\frac{s}{t}\right)^2 + 0.3 E \frac{s}{r}\right)$$

except for cylinders 9, 10, and 11, with large  $\phi$ , where the experimental exceeded the calculated figures by as much as 35 percent.

## b) Wrinkling and Carrying Capacity

Small  $\phi$  ( $\phi = 2.5^\circ, 5^\circ, 8.5^\circ$ ) were accompanied by ar-

bitrary oppositely staggered wrinkles. With increasingly exceeding critical stress, secondary buckles, usually starting at the edge of the sheet, manifested themselves. Further increasing edge stress was followed by sudden bulge rearrangement accompanied by a reduction in effective width, as illustrated in figure 7 for cylinders 1 and

2 at  $\frac{\sigma_R}{\sigma_k} = 7.5$  and  $= 5$ , respectively. The test values for both cylinders is on the average in good agreement with equation (4) and very good for cylinder 3.

At medium  $\varphi$  ( $\varphi = 13^\circ$  and  $30^\circ$ ) and slightly exceeded buckling stress, all panels disclosed only one inwardly directed bulge, which, however, was also followed by secondary bulges as the buckling stress was increasingly exceeded, although to a lesser extent than for the originally slightly curved sheets (figs. 8 and 9). There was no reversal of bulges for  $\varphi = 30^\circ$ . Cylinder No. 6 disclosing a comparatively flat course of the effective width, evinced no secondary bulges even after markedly exceeded buckling stress. The carrying capacity of cylinders 4, 7, and 8, with the same  $\varphi$  but different wall thicknesses ( $s = 0.036$  cm and  $s = 0.052$  cm) showed good agreement with equation (4).

Cylinder No. 5 disclosed a marked reduction in carrying capacity as a result of additional prebulges produced during riveting, as seen in figure 10 and 11, especially on the section at the right. They also show their not inconsiderable effect on the secondary bulges near the edge.

At great  $\varphi$  ( $\varphi = 65^\circ$  and  $113^\circ$ ) the experiments showed severe bulging (fig. 12, cylinder No. 11, correspond to  $\varphi = 113^\circ$ ). As regards the carrying capacity, cylinder No. 10 gave only one test point, while on cylinders Nos. 9 and 11 sheet and section buckled simultaneously.

### c) Form of Failure

On all cylinders the failure of the edge section occurred in the plastic range directly adjacent to the principal bulges (figs. 10 and 11).

## APPENDIX

In the DVL five test specimens (reference 2) (panels) of duralumin with section stiffeners on one side were compressed according to figure 13 over fitted-on clamping rails. The stresses were recorded during the tests at various points of the sheet ( $\sigma_R$ ) and on the stiffening sections ( $\sigma_{mp}$ ) with tensiometers according to arrangement in figure 13. The records disclosed additional bending stresses on the sections of all panels.

These DVL tests were also used to check equation (4) The effective width  $2 b_R$  was computed from the DVL data and plotted in figure 14 for comparison with equation (4) (solid curve).

The panels 2, 3, and 4 with different  $\frac{l}{t}$  values (2.5 and 5.2) manifest good agreement with equation (4). While panel 5 with outside stiffener sections and especially panel 1 give surprisingly high values for the effective width. In these two panels the supplementary bending stresses were especially high. The discrepancies between the DVL test data and equation (4) is probably traceable to the fact that in connection with this bending the shortening of the panel in the median zone was not the same as that on its edge.

Translation by J. Vanier,  
National Advisory Committee  
for Aeronautics.

## REFERENCES

1. Lahde, R., and Wagner, H.: Experimental Studies of the Effective Width of Buckled Sheets. T.M. No. 814, N.A.C.A., 1936.
2. Ebnor, H.: The Strength of Shell Bodies - Theory and Practice. T.M. No. 838, N.A.C.A., 1937.

TABLE I. Dimensions and Buckling Stresses of the Test Cylinders (in cm, kg units)

Identification	Test cylinders											
	1	2	3	4	5	6	7	8	9	10	11	
Angle at center . . . . . $\phi$	2.5°	5°	8.5°	13°	13°	19.5°	30°	30°	65°	66°	113°	
Curvature radius. . . . . r	410	248	180	103	120	53	54	57	29	25	17.8	
Sheet panel {	length . . . . . l	47.4	55.0	57.5	58.5	65.7	45	70	70	82	70	86
	width. . . . . t	18.7	21.7	27	23.4	27	18	28	30	33	28.8	35
	thickness. . . . . s	0.101	0.080	0.062	0.081	0.042	0.072	0.036	0.052	0.045	0.05	0.041
Ratio of {	. . . . . l/t	2.54	2.53	2.5	2.5	2.5	2.5	2.5	2.33	2.49	2.43	2.46
	. . . . . r/s	4060	3100	2900	1270	2845	730	1500	1090	644	500	430
	. . . . . t/s	185	270	435	289	643	250	780	577	730	576	855
Thickness of section. . . . . $s_s$	0.062	0.061	0.042	0.062	0.031	0.050	0.030	0.035	0.035	0.035	0.035	
Total area of cylinder. . . $F_Z$	8.73	8.04	6.85	8.62	4.92	6.36	4.32	6.4	6.1	6.06	5.98	
Proportion of sheet in percent of	} . $F_Z$	64.8	64.9	69.7	66.3	70.3	62.1	70.8	73.1	73.4	72.2	72.6
Proportion of section in percent of		35.2	35.1	30.3	33.7	29.7	37.9	29.2	26.9	26.6	27.8	27.4
Buckling stress of flat sheet. . . . . $\sigma_{\phi b}$	155	73	26	62	13	83	9	16	10	16	7	
Increase in stress due to curvature . . . . . $\sigma_{kr}$	78	103	110	244	109	423	206	284	493	636	738	
Buckling stress of curved sheet . . . . . $\sigma_K$	233	176	136	306	122	506	215	300	503	652	745	
Experimentally defined buckling stress. . . . . $\sigma_{K_V}$	220	170	107	370	131	560	190	320	660	820	800	

N.A.C.A. Technical Memorandum No. 880 8

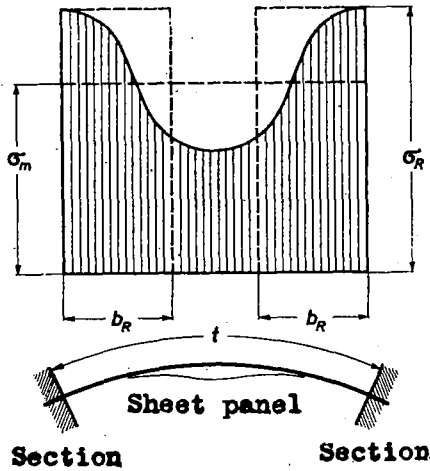


Figure 1.- Stress distribution over panel width t.

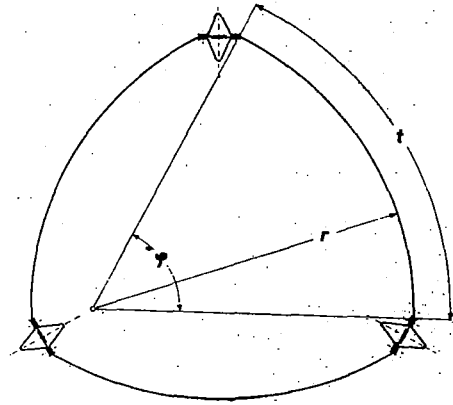


Figure 2.- Section of a test cylinder.

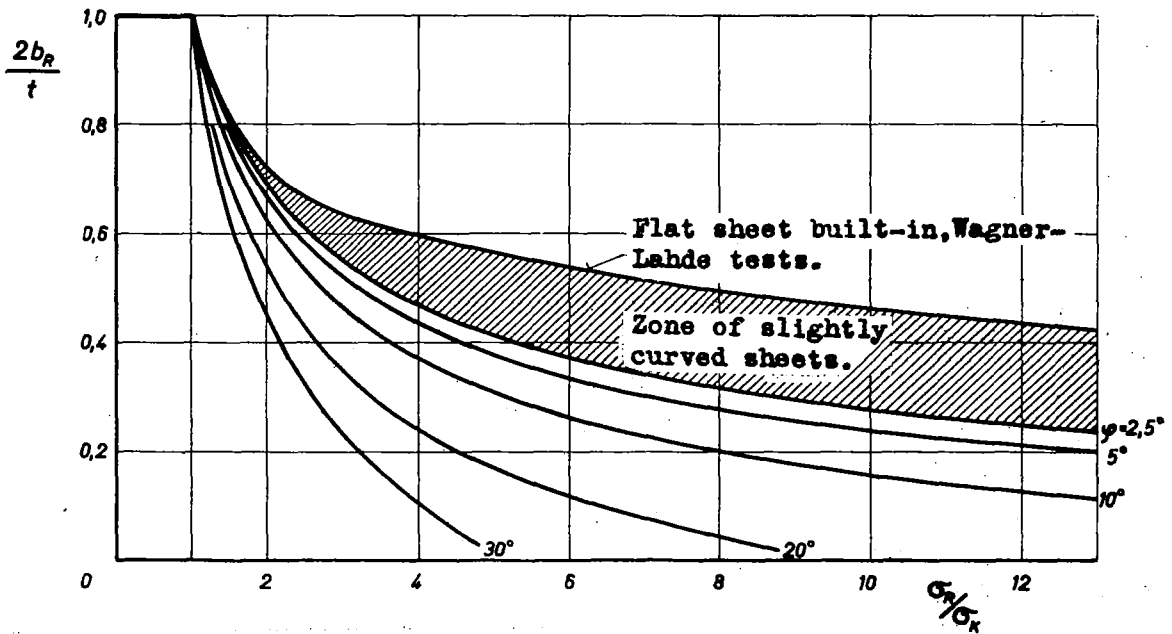


Figure 3.- The effective width for flat and circular curved sheets plotted against the degree of exceeded buckling stress (nondimensional presentation).

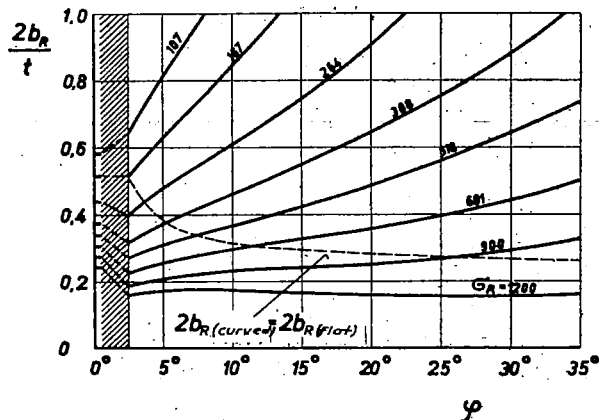


Figure 4.- The effective width for identical edge stresses plotted against  $\varphi$  (ratio of sheet width to wall thickness:  $\frac{t}{b} = 500$ , (material: brass).

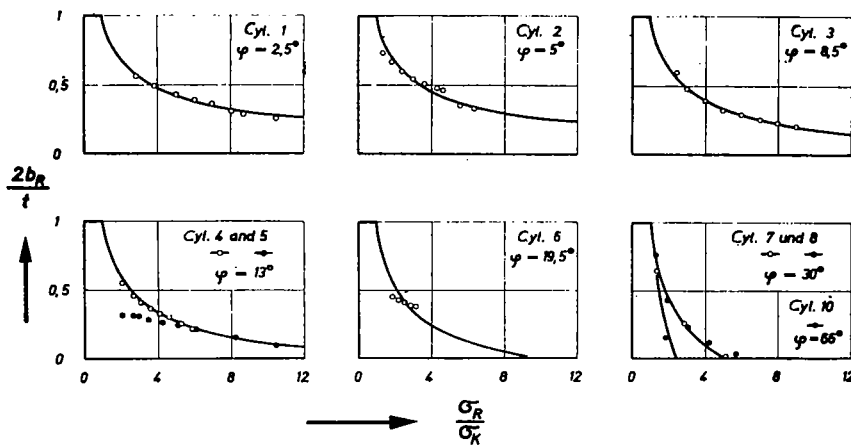


Figure 7.- Test data for the effective width arranged according to  $\varphi$ .

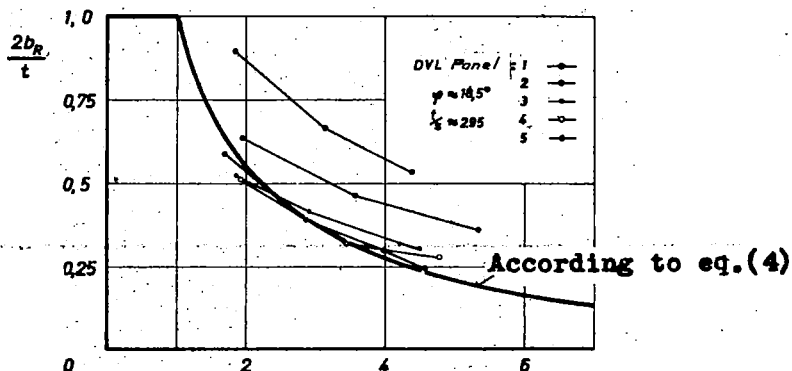


Figure 14.- Comparison of the DVL data with the data for the effective width according to eq.(4).

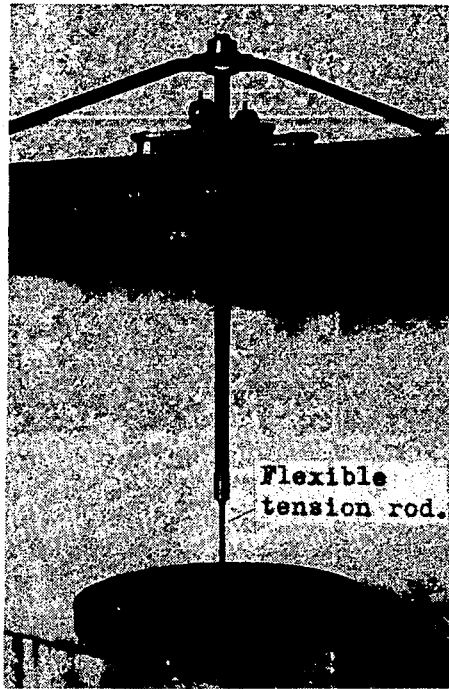


Figure 5.- Test arrangement.



Figure 8.- Test cylinder no. 4  
at  $\sigma_R/\sigma_K = 2.48$



Figure 9.- Test cylinder no. 4  
at  $\sigma_R/\sigma_K = 5$ .

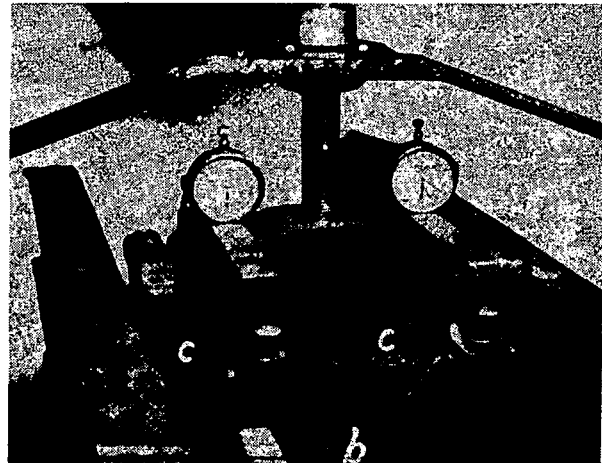


Figure 6.- Setup for determining  
the test load.  
b-Knife edges.  
Springs c mounted on b.



Figure 10.- Test cylinder no.5  
at  $\sigma_R/\sigma_K=4.63$



Figure 11.- Test cylinder no.5  
(form of failure)

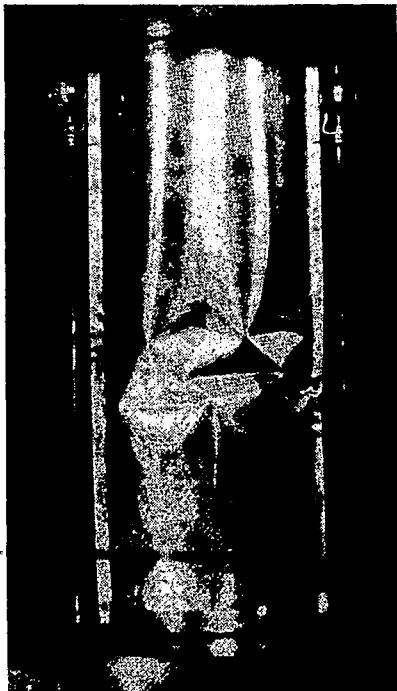


Figure 12.- Test cylinder no.11  
(form of failure)

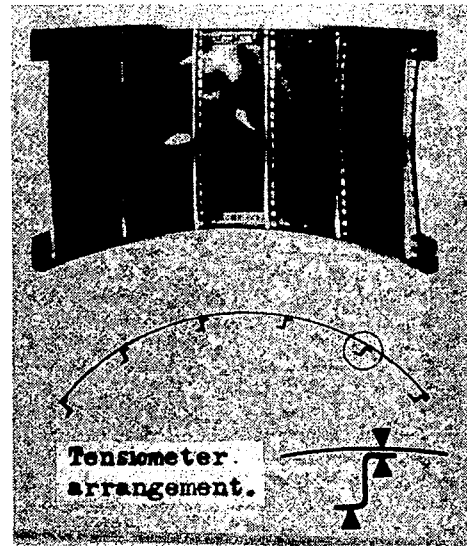


Figure 13.- DVL test arrangement.

NASA Technical Library



3 1176 01440 3605